UK-04-25

Three-Loop Radiative-Recoil Corrections to Hyperfine Splitting in Muonium

Michael I. Eides*

Department of Physics and Astronomy,
University of Kentucky, Lexington, KY 40506, USA, and

Petersburg Nuclear Physics Institute,
Gatchina, St.Petersburg 188350, Russia

Howard Grotch†

Department of Physics and Astronomy,
University of Kentucky, Lexington, KY 40506, USA

Valery A. Shelyuto‡

D. I. Mendeleev Institute of Metrology, St.Petersburg 198005, Russia

Abstract

We consider three-loop radiative-recoil corrections to hyperfine splitting in muonium. These corrections are enhanced by the large logarithm of the electron-muon mass ratio. The leading logarithm cubed and logarithm squared contributions were obtained a long time ago. We calculate the single-logarithmic and nonlogarithmic contributions of order $\alpha^3(m/M)E_F$ generated by gauge invariant sets of diagrams with one- and two-loop polarization insertions in diagrams with two exchanged photons and radiative photons, and by diagrams with one-loop radiative photon insertions both in the electron and muon lines. The results of this paper constitute a next step in the implementation of the program of reduction of the theoretical uncertainty of hyperfine splitting below 10 Hz. They improve the theory of hyperfine splitting, and affect the value of the electron-muon mass ratio extracted from experimental data on the muonium hyperfine splitting.

*Electronic address: eides@pa.uky.edu, eides@thd.pnpi.spb.ru
†Electronic address: hgrotch@uky.edu
‡Electronic address: shelyuto@vniim.ru

I. INTRODUCTION: LEADING LOGARITHMIC CONTRIBUTIONS OF ORDER $\alpha^2(Z\alpha)(m/M)\widetilde{E}_F$

The radiative-recoil corrections of order $\alpha^2(Z\alpha)(m/M)\widetilde{E}_F$[1] to hyperfine splitting in muonium are enhanced by the large logarithm of the electron-muon mass ratio cubed [1]. The leading logarithm cube contribution is generated by the graphs in Fig. 1 [2] with insertions of the electron one-loop polarization operators in the two-photon exchange graphs. It may be obtained almost without any calculations by substituting the effective charge $\alpha(M)$ in the leading recoil correction of order $(Z\alpha)(m/M)\widetilde{E}_F$, and expanding the resulting expression in the power series over α [2].

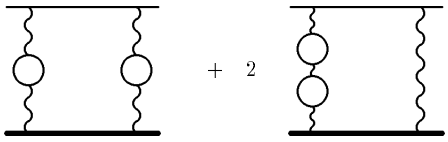

FIG. 1: Graphs with two one-loop polarization insertions

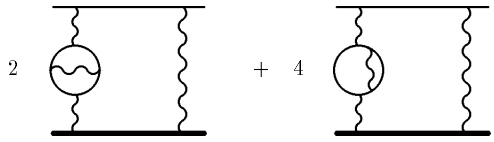

FIG. 2: Graphs with two-loop polarization insertions

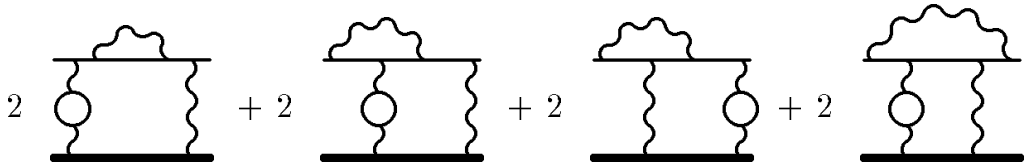

FIG. 3: Graphs with radiative photon insertions

[1] We define the Fermi energy as

$$\widetilde{E}_F = \frac{16}{3} Z^4 \alpha^2 \frac{m}{M} \left(\frac{m_r}{m}\right)^3 ch\, R_\infty, \tag{1}$$

where m and M are the electron and muon masses, α is the fine structure constant, c is the velocity of light, h is the Planck constant, R_∞ is the Rydberg constant, and Z is the nucleus charge in terms of the electron charge ($Z = 1$ for muonium). The Fermi energy $\widetilde{E}_F$ does not include the muon anomalous magnetic moment a_μ which does not factorize in the case of recoil corrections, and should be considered on the same grounds as other corrections to hyperfine splitting.

[2] And by the diagrams with the crossed exchanged photon lines. Such diagrams with the crossed exchanged photon lines are also often omitted in other figures below.

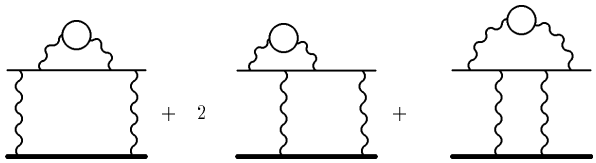

FIG. 4: Graphs with polarization insertions in the radiative photon

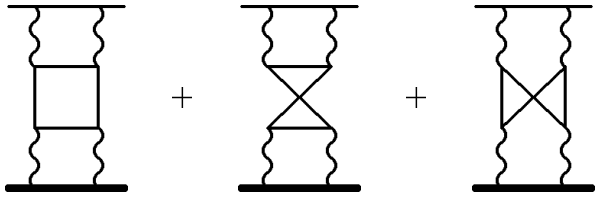

FIG. 5: Graphs with light by light scattering insertions

Calculation of the logarithm squared term of order $\alpha^2(Z\alpha)(m/M)\widetilde{E}_F$ is more challenging [2]. All graphs in Figs. 1, 2, 3, 4, and 5 generate corrections of this order. The contribution induced by the irreducible two-loop vacuum polarization in Fig. 2 is again given by the effective charge expression. Subleading logarithm squared terms generated by the one-loop polarization insertions in Fig. 1 may easily be calculated with the help of the two leading asymptotic terms in the polarization operator expansion and the skeleton integral. The logarithm squared contribution generated by the diagrams in Fig. 3 is obtained from the leading single-logarithmic contribution of the diagrams without polarization insertions by the effective charge substitution. An interesting effect takes place in calculation of the logarithm squared term generated by the polarization insertions in the radiative photon in Fig. 4. One might expect that the high energy asymptote of the electron factor with the polarization insertion is given by the product of the leading constant term of the electron factor $-5\alpha/(4\pi)$ and the leading polarization operator term. However, this expectation turns out to be wrong. One may check explicitly that instead of the naive factor above one has to multiply the polarization operator by the factor $-3\alpha/(4\pi)$. The reason for this effect may easily be understood. The factor $-3\alpha/(4\pi)$ is the asymptote of the electron factor in massless QED and it gives a contribution to the logarithmic asymptotics only after the polarization operator insertion. This means that in massive QED the part $-2\alpha/(4\pi)$ of the constant electron factor originates from the integration region where the integration momentum is of order of the electron mass. Naturally this integration region does not give any contribution to the logarithmic asymptotics of the radiatively corrected electron factor. The least trivial logarithm squared contribution is generated by the three-loop diagrams in Fig. 5 with the insertions of the light by light scattering block. Their contribution was calculated explicitly in [2]. Later it was realized that these contributions are intimately connected with the well known anomalous renormalization of the axial current in QED [3]. Due to the projection on the HFS spin structure in the logarithmic integration region, the heavy particle propagator effectively shrinks to an axial current vertex, and in this situation calculation of the respective contribution to HFS reduces to substitution of the well known two-loop axial renormalization factor in Fig. 6 [4] in the recoil skeleton diagram. As expected, this calculation reproduces the same contribution as obtained by direct calculation of the diagrams with light by light scattering expressions. From the theoretical point of view it is

interesting that one can measure anomalous two-loop renormalization of the axial current in the atomic physics experiment.

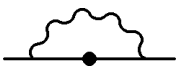

FIG. 6: Renormalization of the fifth current

The sum of all logarithm cubed and logarithm squared contributions of order $\alpha^2(Z\alpha)(m/M)\widetilde{E}_F$ is given by the expression [1, 2]

$$\Delta E = \left(-\frac{4}{3}\ln^3\frac{M}{m} + \frac{4}{3}\ln^2\frac{M}{m}\right)\frac{\alpha^2(Z\alpha)}{\pi^3}\frac{m}{M}\widetilde{E}_F. \tag{2}$$

It was also shown in [2] that there are no other contributions with the large logarithm of the mass ratio squared accompanied by the factor α^3, even if the factor Z enters in another manner than in the equation above.

Single-logarithmic and nonlogarithmic terms of order $\alpha^2(Z\alpha)(m/M)\widetilde{E}_F$ are generated by all diagrams in Figs. 1-4, by the graphs with the muon polarization loops, by the graphs with polarization and radiative photon insertions in the muon line, and also by the three-loop graphs with radiative photons in the electron and/or muon lines. Below we present our recent results for three-loop single-logarithmic and nonlogarithmic radiative-recoil corrections.

II. TWO-PHOTON EXCHANGE DIAGRAMS. CANCELLATION OF THE ELECTRON AND MUON LOOPS

Calculation of single-logarithmic and nonlogarithmic radiative-recoil corrections of relative order $\alpha^2(Z\alpha)(m/M)$ (and also of orders $(Z^2\alpha)^2(Z\alpha)(m/M)$ and $\alpha(Z^2\alpha)(Z\alpha)(m/M)$) resembles in many respects calculation of the corrections of relative orders $\alpha(Z\alpha)(m/M)$ and $Z^2\alpha(Z\alpha)(m/M)$. It was first discovered in [5, 6] that the contributions of the diagrams with insertions of the electron and muon polarization loops partially cancel, and, hence, it is convenient to treat such diagrams simultaneously[3]. Similar cancellation holds also for the corrections of order $\alpha^2(Z\alpha)(m/M)\widetilde{E}_F$, so we will first remind the reader how it arises when one calculates the polarization contribution of order $\alpha(Z\alpha)(m/M)\widetilde{E}_F$. The recoil contribution in the heavy particle pole of the two-photon exchange diagrams exactly cancels in the sum of the electron and muon polarizations (see for more details [6, 7]). Then the skeleton recoil contribution to the hyperfine splitting generated by the diagrams with two-photon exchanges in Fig. 7 is the result of the subtraction of the heavy pole contribution

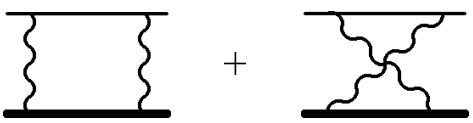

[3] We always consider the external muon as a particle with charge Ze, this makes the origin of different contributions more transparent. However, somewhat inconsequently we omit the factor Z in the case of the closed muon loops. The reason for this apparent inconsistency is just the cancellation which we discuss now.

FIG. 7: Diagrams with two-photon exchanges

$$\Delta E = 4\frac{Z\alpha}{\pi}\frac{m}{M}\widetilde{E}_F\int_0^\infty \frac{dk}{k}\left[f(\mu k) - f\left(\frac{k}{2}\right)\right], \tag{3}$$

where $\mu = m/(2M)$, and

$$f(k) = \frac{1}{k}\left(\sqrt{1+k^2} - k - 1\right) - \frac{1}{2}\left(k\sqrt{1+k^2} - k^2 - \frac{1}{2}\right), \tag{4}$$

$$f(k)_{k\to 0} \to -\frac{3}{4} + \frac{k^2}{2}, \qquad f(k)_{k\to\infty} \to -\frac{1}{k}.$$

The electron polarization contribution is obtained from the skeleton integral by multiplying the expression in eq.(3) by the multiplicity factor 2, and inserting the polarization operator $(\alpha/\pi)k^2 I_1(k)$ in the integrand

$$\frac{\alpha}{\pi}k^2 I_1(k) \equiv \frac{\alpha}{\pi}k^2\int_0^1 dv \frac{v^2(1-v^2/3)}{4+k^2(1-v^2)}. \tag{5}$$

The muon polarization contribution is given by a similar expression, and the total recoil contribution induced by the diagrams with both the one-loop electron and muon polarizations in Fig. 8 has the form

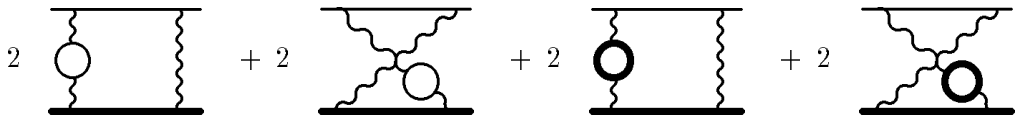

FIG. 8: Diagrams with one-loop polarization insertions

$$\Delta E = 8\frac{\alpha(Z\alpha)}{\pi^2}\frac{m}{M}\widetilde{E}_F\int_0^\infty \frac{dk}{k}\left[f(\mu k) - f\left(\frac{k}{2}\right)\right][k^2 I_1(k) + k^2 I_{1\mu}(k)]. \tag{6}$$

One can simplify this integral and demonstrate that with linear accuracy in the small mass ratio m/M all recoil contributions generated by the diagrams with the one-loop electron and muon polarization insertions in Fig. 8 are given by the integral

$$\Delta E = 8\frac{\alpha(Z\alpha)}{\pi^2}\frac{m}{M}\widetilde{E}_F\int_0^\infty \frac{dk}{k} f(\mu k)k^2 I_1(k). \tag{7}$$

This integral was calculated in [6] and we will not discuss its calculation here. Our only goal in this Section was to demonstrate the mechanism of the partial cancellation of the electron loop and muon loop contributions.

III. DIAGRAMS WITH EITHER TWO ELECTRON OR TWO MUON LOOPS

The nonrecoil contribution generated by the diagrams with two electron or muon loops in Fig. 1 and Fig. 9 was obtained a long time ago [8]. Although it was not emphasized in that work explicitly, it is easy to check that the result in [8] includes heavy pole contributions

which are due to the diagrams with both the electron and muon polarizations. Repeating the same steps as in the previous Section, it is easy to see that the recoil contribution generated by the diagrams in Fig. 1 and Fig. 9 is determined by the integral

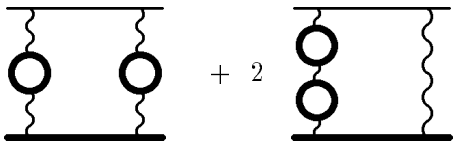

FIG. 9: Graphs with two muon one-loop polarization insertions

$$\Delta E = 12\frac{\alpha^2(Z\alpha)}{\pi^3}\frac{m}{M}\widetilde{E}_F\int_0^\infty \frac{dk}{k} f(\mu k) k^4 I_1^2(k), \tag{8}$$

where the numerical factor before the integral is due to the multiplicity of the diagrams, and the whole integral is similar to the integral in eq.(7). The only significant difference is that now we have the two-loop factor $k^4 I^2(k)$ in the integrand instead of the one-loop factor $k^2 I_1(k)$. Calculating this integral we obtain the total recoil contribution generated by the diagrams in Fig. 1 and Fig. 9 [9]

$$\Delta E = \left[-\frac{4}{3}\ln^3\frac{M}{m} - \frac{8}{3}\ln^2\frac{M}{m} - \left(\frac{2\pi^2}{3}+\frac{25}{9}\right)\ln\frac{M}{m} - \frac{4\pi^2}{9} - \frac{535}{108}\right]\frac{\alpha^2(Z\alpha)}{\pi^3}\frac{m}{M}\widetilde{E}_F. \tag{9}$$

The logarithm cube and logarithm squared terms in this expression were obtained in [1, 2].

IV. DIAGRAMS WITH BOTH THE ELECTRON AND MUON LOOPS

Consider now the diagrams with one electron and one muon loop in Fig. 10. We can look at these diagrams as a result of the electron polarization operator insertions in the muon loop diagrams in Fig. 8. The complete analytic expression for the last two diagrams in Fig. 8 has the form

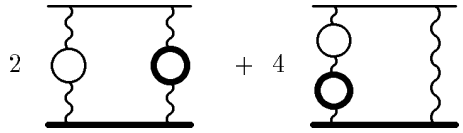

FIG. 10: Graphs with both the electron and muon loops

$$\Delta E = 8\frac{\alpha(Z\alpha)}{\pi^2}\frac{m}{M}\widetilde{E}_F\int_0^\infty \frac{dk}{k}\left[\widetilde{f}(\mu k) - \widetilde{f}\left(\frac{k}{2}\right)\right] k^2 I_{1\mu}(k), \tag{10}$$

where

$$\widetilde{f}(k) = f(k) + \frac{1}{k}.$$

After calculations we obtain [9]

$$\Delta E = \left[\left(\frac{2\pi^2}{3} - \frac{20}{9}\right)\ln\frac{M}{m} + \frac{\pi^2}{3} - \frac{53}{9}\right]\frac{\alpha^2(Z\alpha)}{\pi^3}\frac{m}{M}\widetilde{E}_F. \tag{11}$$

V. DIAGRAMS WITH SECOND ORDER POLARIZATION INSERTIONS

The recoil contribution to HFS generated by the diagrams in Fig. 2 and Fig. 11 with two-loop electron and muon polarization insertions is given by the integral (compare eq.(7))

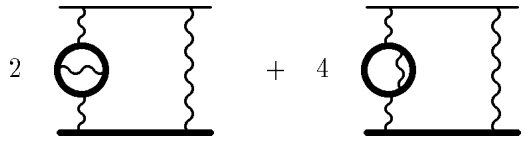

FIG. 11: Graphs with muon two-loop polarization insertions

$$\Delta E = 8\frac{\alpha^2(Z\alpha)}{\pi^3}\frac{m}{M}\widetilde{E}_F\int_0^\infty\frac{dk}{k}f(\mu k)k^2I_2(k), \tag{12}$$

where $(\alpha^2/\pi^2)k^2I_2(k)$ is the two-loop polarization operator [10, 11]

$$\begin{aligned} I_2(k) = \frac{2}{3}\int_0^1 dv\frac{v}{4+k^2(1-v^2)}\Bigg\{&(3-v^2)(1+v^2)\left[\mathrm{Li}_2\left(-\frac{1-v}{1+v}\right)\right. \\ &\left.+2\mathrm{Li}_2\left(\frac{1-v}{1+v}\right)+\frac{3}{2}\ln\frac{1+v}{1-v}\ln\frac{1+v}{2}-\ln\frac{1+v}{1-v}\ln v\right] \\ &+\left[\frac{11}{16}(3-v^2)(1+v^2)+\frac{v^4}{4}\right]\ln\frac{1+v}{1-v} \\ &+\left[\frac{3}{2}v(3-v^2)\ln\frac{1-v^2}{4}-2v(3-v^2)\ln v\right]+\frac{3}{8}v(5-3v^2)\Bigg\}. \end{aligned} \tag{13}$$

The integral in eq.(12) admits an analytic calculation and the recoil contribution to HFS generated by the diagrams with two-loop polarization insertions in Fig. 11 turns out to be [9]

$$\begin{aligned} \Delta E = \Bigg\{&-\frac{3}{2}\ln^2\frac{M}{m}-\left[6\zeta(3)+\frac{13}{4}\right]\ln\frac{M}{m}-\frac{97}{8}\zeta(3)-16\mathrm{Li}_4\left(\frac{1}{2}\right) \\ &+\frac{2\pi^2}{3}\ln^2 2-\frac{2}{3}\ln^4 2+\frac{5\pi^4}{36}-\frac{\pi^2}{4}+\frac{7}{16}\Bigg\}\frac{\alpha^2(Z\alpha)}{\pi^3}\frac{m}{M}\widetilde{E}_F, \end{aligned} \tag{14}$$

where $\zeta(3) = 1.2020569\ldots$ and $\mathrm{Li}_4(1/2) = 0.517479\ldots$. The logarithm squared term in this expression was obtained in [2].

VI. LEADING FOUR-LOOP RADIATIVE-RECOIL CORRECTION

This leading four-loop radiative-recoil correction is generated by the diagrams with four polarization operator insertions in the exchanged photons similar to the diagrams with the three polarization insertions in Fig. 1. It contains the large logarithm to the fourth power, and like the leading logarithm cubed contribution in Eq.(2) may be easily obtained either by direct calculation or by substitution of the effective charge $\alpha(M)$ in the leading recoil correction of order $(Z\alpha)(m/M)\widetilde{E}_F$ [9]

$$\Delta E = -\frac{8}{9}\ln^4\frac{M}{m}\frac{\alpha^3(Z\alpha)}{\pi^4}\,\frac{m}{M}\widetilde{E}_F. \tag{15}$$

We consider this correction of order $\alpha^3(Z\alpha)$ together with the radiative-recoil corrections of order $\alpha^2(Z\alpha)$ because, due to the presence of the large logarithm, it is numerically of the same order as these corrections

$$\Delta E = -\,1.\,668\,\frac{\alpha^2(Z\alpha)}{\pi^3}\frac{m}{M}\widetilde{E}_F. \tag{16}$$

VII. DIAGRAMS WITH RADIATIVE PHOTONS IN THE ELECTRON LINE

A. Electron Vacuum Polarization

Now we turn to consideration of diagrams which include both the radiative photon insertions in the electron and/or muon line and the polarization insertions in the exchanged photons. There are four gauge invariant sets of such three-loop diagrams, and we calculate all their contributions.

All these four sets of diagrams can be obtained from the two-photon exchange diagrams in Fig. 12 and in Fig. 13 with the radiative photons in the electron or muon lines by insertions of the one-loop electron or muon polarization operators.

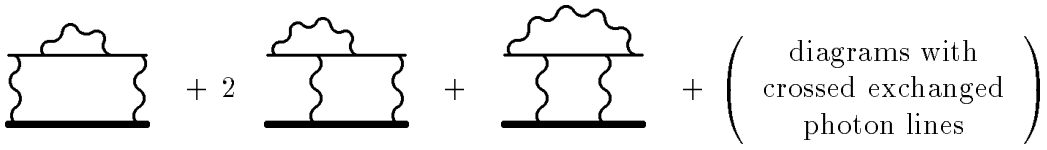

FIG. 12: Electron-line radiative-recoil corrections

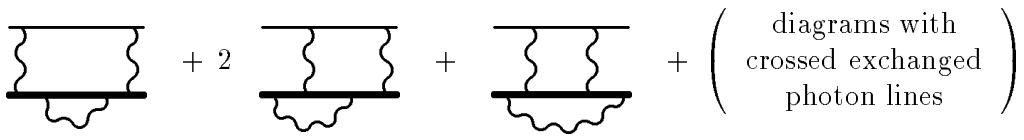

FIG. 13: Muon-line radiative-recoil corrections

We have derived earlier a relatively compact integral representation for the radiative-recoil corrections generated by the diagrams in Fig. 12 and in Fig. 13 [12, 13] (these integral representations do not include anomalous magnetic moments of the electron and muon,

respectively). The explicit expression for this integral representation is too cumbersome to reproduce it here. The expression for the contribution to HFS arising from the diagrams in Fig. 14 is obtained from the integral in [12, 13] by insertion in the integrand of the doubled one-loop electron polarization $(\alpha/\pi)k^2 I_e(k)$

$$2\left(\frac{\alpha}{\pi}\right)k^2 I_e(k) = 2\left(\frac{\alpha}{\pi}\right)k^2 \int_0^1 dv \frac{v^2(1-v^2/3)}{4+k^2(1-v^2)}, \tag{17}$$

where the additional multiplicity factor 2 corresponds to the fact that we can insert the vacuum polarization in each of the exchanged photons.

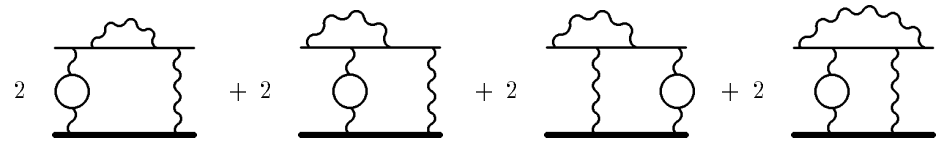

FIG. 14: Electron line and electron vacuum polarization

Calculating the respective integral we obtain the radiative-recoil correction of order $\alpha^2(Z\alpha)(m/M)\widetilde{E}_F$ generated by the diagrams in Fig. 14 (with the electron anomalous magnetic moment subtracted) [14]

$$\Delta E = \left[\frac{5}{2}\ln^2\frac{M}{m} + \frac{22}{3}\ln\frac{M}{m} + 11.41788\ (3)\right]\frac{\alpha^2(Z\alpha)}{\pi^3}\frac{m}{M}\widetilde{E}_F. \tag{18}$$

B. Muon Vacuum Polarization

Let us consider now the diagrams in Fig. 15. The only difference between these diagrams and the diagrams in Fig. 14 from the previous section is that they contain the muon vacuum polarization insertion

$$2\left(\frac{\alpha}{\pi}\right)k^2 I_\mu(k) = 2\left(\frac{\alpha}{\pi}\right)k^2 \int_0^1 dv \frac{v^2(1-v^2/3)}{\mu^{-2}+k^2(1-v^2)}, \tag{19}$$

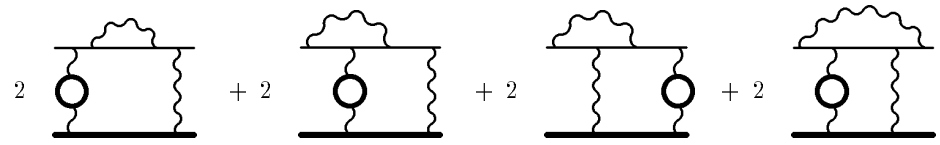

FIG. 15: Electron line and muon vacuum polarization

instead of the electron vacuum polarization.

After calculations we obtain the contribution of the diagrams in Fig. 15 (with the electron anomalous magnetic moment subtracted) [14]

$$\Delta E = \left[-\frac{5\pi^2}{12} + \frac{1}{18}\right]\frac{\alpha^2(Z\alpha)}{\pi^3}\frac{m}{M}\widetilde{E}_F. \tag{20}$$

C. Electron Anomalous Magnetic Moment and Vacuum Polarizations

It is well known that the electron anomalous magnetic moment formally present in the diagrams in Fig. 12 does not produce any contribution to the recoil corrections of order $\alpha(Z\alpha)(m/M)\widetilde{E}_F$ [6, 15, 16]. This is the reason why the integral representation [12, 13] used above to calculate the corrections generated by the diagrams in Fig. 14 and in Fig. 15 does not include the anomalous magnetic moment contributions. Such contributions connected with these diagrams should be considered separately. As we discussed in Section II there is a partial cancellation between the electron and muon loops in the corrections with insertions of polarization loops in the exchanged photons in Fig. 8. We expect similar partial cancellation in the electron anomalous magnetic moment contributions generated by the diagrams in Fig. 14 and in Fig. 15, and therefore consider the correction generated by the sum of these diagrams. After calculations, we obtain an analytic result for the electron anomalous magnetic moment contributions in Fig. 14 and in Fig. 15

$$\Delta E = \left[-4\ln\frac{M}{m} + \frac{4}{3}\right]\frac{\alpha^2(Z\alpha)}{\pi^3}\frac{m}{M}\widetilde{E}_F. \tag{21}$$

VIII. DIAGRAMS WITH RADIATIVE PHOTONS IN THE MUON LINE

A. Muon Vacuum Polarization

The contribution to the energy shift generated by the diagrams in Fig. 16 is obtained from the expression for the diagrams in Fig. 13 by insertion in the integrand of the doubled muon vacuum polarization

$$2\left(\frac{\alpha}{\pi}\right)k^2 I_\mu(k) = 2\left(\frac{\alpha}{\pi}\right)k^2\int_0^1 dv\frac{v^2(1-v^2/3)}{4+k^2(1-v^2)}. \tag{22}$$

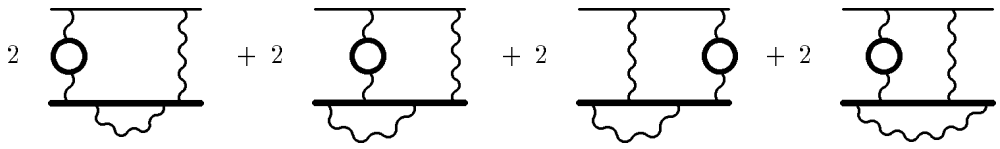

FIG. 16: Muon line and muon vacuum polarization

After calculations, we obtain the contribution to HFS generated by the diagrams in Fig. 16 (with the muon anomalous magnetic moment subtracted) [14]

$$\Delta E = -1.\ 80176\ (2)\frac{\alpha(Z^2\alpha)(Z\alpha)}{\pi^3}\frac{m}{M}\widetilde{E}_F. \tag{23}$$

B. Electron Vacuum Polarization

Let us turn now to the diagrams in Fig. 17. The only difference between these diagrams and the diagrams in Fig. 16 is that now we have electron polarization insertions instead of the muon polarization insertions.

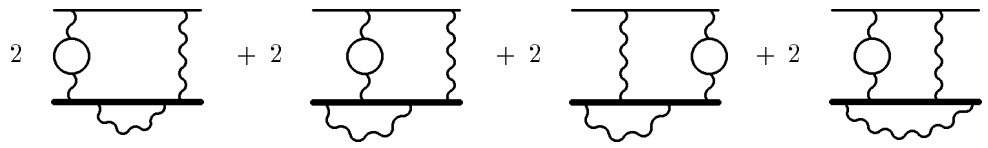

FIG. 17: Muon line and electron vacuum polarization

The contribution to HFS generated by the diagrams in Fig. 17 (with the muon anomalous magnetic moment subtracted) is equal to [14]

$$\Delta E = \left[\left(6\zeta(3) - 4\pi^2 \ln 2 + \frac{13}{2}\right)\ln\frac{M}{m} + 24.32115\ (4)\right]\frac{\alpha(Z^2\alpha)(Z\alpha)}{\pi^3}\frac{m}{M}\widetilde{E}_F. \qquad (24)$$

C. Muon Anomalous Magnetic Moment and Vacuum Polarizations

Consider now muon anomalous magnetic moment contributions generated by the diagrams in Fig. 16 and in Fig. 17. As in the case of radiative insertions in the electron line, we expect partial cancellation (for more details see [17]) and consider corrections generated by the sum of these diagrams. After calculations, we obtain an analytic result for the muon anomalous magnetic moment contributions in Fig. 16 and in Fig. 17

$$\Delta E = \left[-4\ln\frac{M}{m} + \frac{4}{3}\right]\frac{\alpha(Z^2\alpha)(Z\alpha)}{\pi^3}\frac{m}{M}\widetilde{E}_F. \qquad (25)$$

IX. THREE-LOOP CORRECTIONS GENERATED BY ONE-LOOP FERMION FACTORS

Consider three-loop radiative-recoil corrections to hyperfine splitting in muonium generated by the diagrams in Fig. 18. These corrections are nonlogarithmic and, unlike the case of the radiative-recoil corrections of orders $\alpha(Z\alpha)(m/M)\widetilde{E}_F$ and $(Z^2\alpha)(Z\alpha)(m/M)\widetilde{E}_F$, the one-loop anomalous magnetic moments of both particles give nonvanishing contributions to these diagrams. We use for calculations explicit expressions for the subtracted electron and muon factors obtained earlier [12, 13].

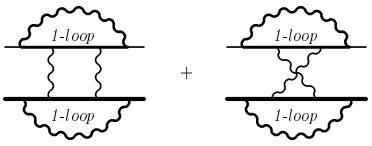

FIG. 18: Diagrams with two fermion factors

After tedious calculations, we obtain an analytic result for the three-loop radiative-recoil correction to hyperfine splitting in muonium generated by the diagrams in Fig. 18 [18]

$$\Delta E = \left[-\frac{15}{8}\zeta(3) + \frac{15\pi^2}{4}\ln 2 + \frac{27\pi^2}{16} - \frac{147}{32}\right]\frac{\alpha(Z^2\alpha)(Z\alpha)}{\pi^3}\frac{m}{M}\ \widetilde{E}_F. \qquad (26)$$

X. DISCUSSION OF RESULTS

Combining all three-loop single-logarithmic and nonlogarithmic corrections to hyperfine splitting in eq.(11), eq.(14), eq.(16), eq.(18), eq.(20), eq.(21) eq.(23), eq.(24), eq.(25), and eq.(26) we obtain ($Z = 1$ below)

$$\Delta E_{tot} = \left[\left(-4\pi^2 \ln 2 - \frac{29}{12}\right) \ln \frac{M}{m} - 14\zeta(3) - 16\mathrm{Li}_4\left(\frac{1}{2}\right) + \frac{2\pi^2}{3} \ln^2 2 \right. \tag{27}$$
$$\left. + \frac{15\pi^2}{4} \ln 2 - \frac{2}{3} \ln^4 2 + \frac{5\pi^4}{36} + \frac{191\pi^2}{144} - \frac{10655}{864} + 29.88049\ (6)\right] \frac{\alpha^3}{\pi^3} \frac{m}{M}\ \widetilde{E}_F,$$

or

$$\Delta E_{tot} = \left[\left(-4\pi^2 \ln 2 - \frac{29}{12}\right) \ln \frac{M}{m} + 47.7213\right] \frac{\alpha^3}{\pi^3} \frac{m}{M}\ \widetilde{E}_F. \tag{28}$$

Numerically this contribution to the muonium HFS is

$$\Delta E_{tot} = -0.030\ 4\ \mathrm{kHz}. \tag{29}$$

Currently the theoretical accuracy of hyperfine splitting in muonium is about 70 Hz. A realistic goal is to reduce this uncertainty below 10 Hz (see a more detailed discussion in [7, 14]). The contributions discussed above, eq.(26), together with the results of other recent research [13, 19, 20] makes achievement of this goal closer. Phenomenologically, the improved accuracy of the theory of hyperfine splitting would lead to a reduction of the uncertainty of the value of the electron-muon mass ratio derived from the experimental data [21] on hyperfine splitting (see, e.g., reviews in [7, 22]).

The single-logarithmic and nonlogarithmic three-loop radiative-recoil corrections generated by the gauge invariant sets of diagrams with two-loop fermion factors and light-by-light insertions in the exchanged photons remain to be calculated. Work on their calculation is in progress now.

Acknowledgments

This work was supported in part by the NSF grant PHY-0138210. The work of V. A. Shelyuto was also supported in part by the RFBR grants 03-02-04029 and 03-02-16843 and DFG grant GZ 436 RUS 113/769/0-1.

---

[1] M. I. Eides and V. A. Shelyuto, Phys. Lett. **146B**, 241 (1984).
[2] M. I. Eides, S. G. Karshenboim, and V. A. Shelyuto, Phys. Lett. **216B**, 405 (1989); Yad. Fiz. **49**, 493 (1989) [Sov. J. Nucl. Phys. **49**, 309 (1989)].
[3] S. G. Karshenboim, M. I. Eides, and V. A. Shelyuto, Yad. Fiz. **52**, 1066 (1990) [Sov. J. Nucl. Phys. **52** (1990) 679].
[4] S. L. Adler, Phys. Rev. **177**, 2426 (1969).
[5] E. A. Terray and D. R. Yennie, Phys. Rev. Lett. **48**, 1803 (1982).
[6] J. R. Sapirstein, E. A. Terray, and D. R. Yennie, Phys. Rev. **D29**, 2290 (1984).
[7] M. I. Eides, H. Grotch, and V. A. Shelyuto, Phys. Rep. **342**, 63 (2001).

[8] M. I. Eides, S. G. Karshenboim, and V. A. Shelyuto, Phys. Lett. **229B**, 285 (1989); Pis'ma Zh. Eksp. Teor. Fiz. **50**, 3 (1989) [JETP Lett. **50**, 1 (1989)]; Yad. Fiz. **50**, 1636 (1989) [Sov. J. Nucl. Phys.**50**, 1015 (1989)].
[9] M. I. Eides, H. Grotch, and V. A. Shelyuto, Phys. Rev. D **65**, 013003 (2002).
[10] G. Kallen and A. Sabry, Kgl. Dan. Vidensk. Selsk. Mat.-Fis. Medd. **29** (1955) No.17.
[11] J. Schwinger, Particles, Sources and Fields, Vol.2 (Addison-Wesley, Reading, MA, 1973).
[12] V. Yu. Brook, M. I. Eides, S. G. Karshenboim, and V. A. Shelyuto, Phys. Lett. B **216**, 401 (1989).
[13] M. I. Eides, H. Grotch, and V. A. Shelyuto, Phys. Rev. D **58**, 013008 (1998).
[14] M. I. Eides, H. Grotch, and V. A. Shelyuto, Phys. Rev. D **67**, 113003 (2003).
[15] J. R. Sapirstein, E. A. Terray, and D. R. Yennie, Phys. Rev. Lett. **51**, 982 (1983).
[16] M. I. Eides, S. G. Karshenboim, and V. A. Shelyuto, Ann. Phys. (NY) **205**, 231 (1991).
[17] M. I. Eides, S. G. Karshenboim, and V. A. Shelyuto, Ann. Phys. (NY) **205**, 291 (1991).
[18] M. I. Eides, H. Grotch, and V. A. Shelyuto, Phys. Rev. D **70**, 073005 (2004).
[19] K. Melnikov and A. Yelkhovsky, Phys. Rev. Lett. **86**, 1498 (2001).
[20] R. J. Hill, Phys. Rev. Lett. **86**, 3280 (2001).
[21] W. Liu, M. G. Boshier, S. Dhawan et al, Phys. Rev. Lett. **82**, 711 (1999).
[22] P. J. Mohr and B. N. Taylor, Rev. Mod. Phys. **72**, 351 (2000).